ELSEVIER

Forest Ecology and Management 169 (2002) 115-122

Forest Ecology and Management

www.elsevier.com/locate/foreco

Carbon and water exchanges of regenerating forests in central Siberia

M. Meroni[a,*], D. Mollicone[b], L. Belelli[a], G. Manca[a], S. Rosellini[a], S. Stivanello[a], G. Tirone[a], R. Zompanti[a], N. Tchebakova[c], E.D. Schulze[d], R. Valentini[a]

[a] *University of Tuscia, DISAFRI and INFM of Viterbo, Viterbo, Italy*

[b] *Joint Research Centre of the European Commission, Ispra VA, Italy*

[c] *Sukachev Institute of Forest, Krasnoyarsk, Russia*

[d] *Max Planck Institute for Biogeochemistry, Jena, Germany*

Abstract

Direct measurements of CO_2 and water vapour of regenerating forests after fire events (secondary succession stages) are needed to determine the role of such disturbances in the biome carbon and water cycles functioning. An estimation of the extension of burnt areas is also required in order to quantify NBP (net biome productivity), a variable that includes large-scale carbon losses (such as fire) bypassing heterotrophic respiration.

Hence, *eddy covariance* measurements of CO_2 and water vapour were carried out in a natural regenerating forest after a fire event. Measurements were collected continuously over a *Betula* spp. stand in central Siberia during summer 1999. Minimum carbon exchange rate (NEE, net ecosystem exchange) exceeded -30 μmol m^{-2} s^{-1} (net flux negative indicating CO_2 uptake by vegetation) and the partitioning of the available energy was mostly dominated by latent heat flux. Structure, age and composition of the forest were analysed to understand the secondary succession stages. The results were compared with previous studies on coniferous forests where biospheric exchanges of energy were dominated by sensible heat fluxes and small carbon uptake rates, thus indicating rather limiting growing conditions. A classification of a Landsat-4 Thematic Mapper scene has been carried out to determine the magnitude of burnt areas and the extension of broadleaf regenerating forests. Analysis of burnt areas spatial frequency and carbon exchanges of the regenerating forest stress the importance of considering large area disturbances for full carbon accounting.

Keywords: Boreal forests; Fires; Carbon and water exchanges; Eddy covariance; Remote sensing

1. Introduction

It is today well accepted by the scientific community as well as in international treaties (Kyoto Protocol) that the terrestrial biosphere has an important role in the global carbon cycle. It has been suggested that the imbalance between total carbon found in the atmosphere and fossil fuel emissions can be explained by a terrestrial sink of about 2 Gt C per year located in the northern Hemisphere forests (Tans et al., 1990; Schimel, 1995). Forests, in terrestrial vegetation, have the maximum potential of carbon sequestration, contributing about 60% of the total net primary production of terrestrial ecosystems (Melillo et al., 1993)

* Corresponding author. Present address: Laboratorio di Telerilevamento, DISAT, Universita' degli Studi di Milano Bicocca Piazza della Scienza 1, 20126 Milan, Italy. Tel.: +39-0761-357394; fax: +39-0761-357389.

E-mail address: mic@unimi.it (M. Meroni).

PII: S0378-1127(02)00302-X

and play a prominent role in the terrestrial global carbon cycle.

Siberia covers 1280×10^9 ha, of which 48% is forested. These forests constitute about 20% of total world forests and a consistent component of global total net primary production (Shvidenko and Nilsson, 1994). The *Russian Taiga* is the largest forest of the world, extending for 8,865,000 km^2 (Nilsson and Shvidenko, 1997). Recently, a growing interest has been manifested on the possible role of Siberian forests in the global carbon cycle (Shulze et al., 1999). However, these previous studies were mostly concentrating on *Pinus sylvestris* forests of the West region of the Yenisey River. These forests are subject to very limiting growing conditions, i.e. low carbon uptake rates, energy mostly dissipated in sensible heat fluxes as well as a pronounced effect of water stress during summer conditions (Valentini et al., 2000). In the same region there is indeed a mosaic of several types of uniform and mixed boreal forests. The *dark coniferous taiga* is a forest dominating the region East of the Yenisey River, mainly composed by *Abies sibirica* and *Picea obovata,* coniferous tree species with dark green coloured needles. This sort of *taiga* grows on the Yenisey Mountains, from the 57th to the 62nd north parallel and from the 90th to the 92nd east meridian.

Fire represents, together with insects and wind, a major natural disturbance of the *dark coniferous taiga,* but it is only due to its action that the growth of a broadleaf forest can start. After a crown fire an even-aged forest composed mainly by *Betula pendula* and *Populus tremula,* that represent the first stage of the *dark coniferous taiga* secondary succession, persists until it is 100-120 years old. Then, in a short time, sometimes only 10-20 years, it turns into a coniferous forest with a prevalence of *A. sibirica, P. obovata* and *Pinus sibirica.* If any other strong disturbance occurs, these coniferous forests will have at the beginning a low vertical and horizontal diversity, then they will change into uneven-aged mixed forests; again aspens and birches are present, with many gaps and different layers of vegetation in the forest.

With the aim of quantifying the possible role of such early successional forests in the Siberian carbon balance, biospheric exchanges of carbon and energy were measured over a birch forest during summer 1999, following its vegetative period from July to September. The measurements site (60°58'5"N; 89°43'2"E; 200 m a.s.l.) was located closed to the village of Zotino in the region of Krasnoyarsk, which stretches from Mongolian highlands northwards up to the Arctic sea and is wholly crossed by river Yenisey.

A remote sensing analysis was performed to understand the impact of the crown fires on the *dark coniferous taiga* and to quantify the extension of the broadleaf regenerating forests.

2. Materials and methods

2.1. Study site description

The research was conducted on a broadleaf forest, at about 2 km of distance from the Yenisey River (Fig. 1). This forest was generated by a crown fire event in the *dark coniferous taiga*: traces of previous forest were well evident as partially carbonised trunks of conifers remained either standing or downed to the ground. Tree age determination after dendrocronological analyses over the highest trees fixed the time of fire event about 50 years before (the oldest tree resulted 48 years old). Soil and meteorological characteristics of the study site are summarised in Table 1.

Regarding the aerodynamic properties of the stand, the terrain was flat, there was a homogeneous fetch of 1300 m N-S and 600 m W-E, 95% of the trees were shorter than 19 m and the range of heights of the dominant layer was 17-18 m.

In order to study structure and composition of the stand, different sample plots have been analysed:

- a 25 m × 25 m sample plot near the scaffold tower used for *eddy covariance* measurements ('tower plot');
- four transects 10 m wide and 100 m long oriented along cardinal points (directions N, E, S and W from the scaffold tower) covering an area of 4000 m^2 to characterise the forest stand ('transects').

Table 1
Site characterisation (mean values refer to the available measurements period—July and August 1999)

Soil type	Loamy
Permafrost	Not present
Mean daily temperature	18.5 °C
Mean monthly rainfall	32 mm

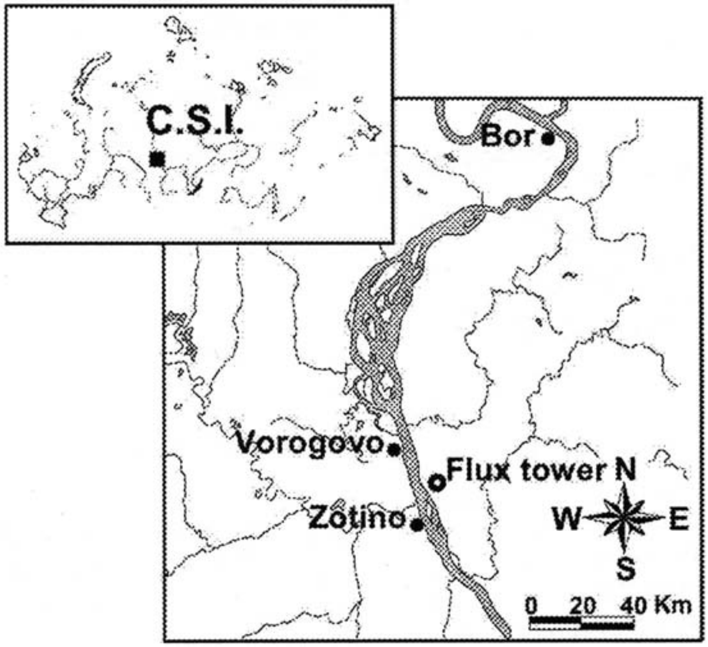

Fig. 1. Study area and location of flux measurements site ('flux tower').

No diametrical threshold was adopted for plant count; stems were measured at 1.30 m of height from the ground (at breast height, b.h.). Consequently, plants shorter than that value were excluded and counted separately as forest regeneration.

The tree species found were *B. pendula, P. tremula* and *Sorbus sibirica,* for hardwoods; *P. obovata, A. sibirica* and *P. sibirica* for conifers.

The most represented species was birch (Fig. 2A), in terms of number, followed by sorb, fir and poplar. Comparing Fig. 2A with Fig. 2B (basal area distribution) it is, however, evident that birch and poplar form the great bulk of biomass of the stand, while the other species occupy the lower story with young plants. Thus the stand can be compared to an almost pure birch forest that shows the first signs of an incoming change in species composition.

Spatial distribution of trees, investigated applying T-square method, resulted uniform (c = 0.0047), density estimation was 2816 plants ha^{-1}, basal area

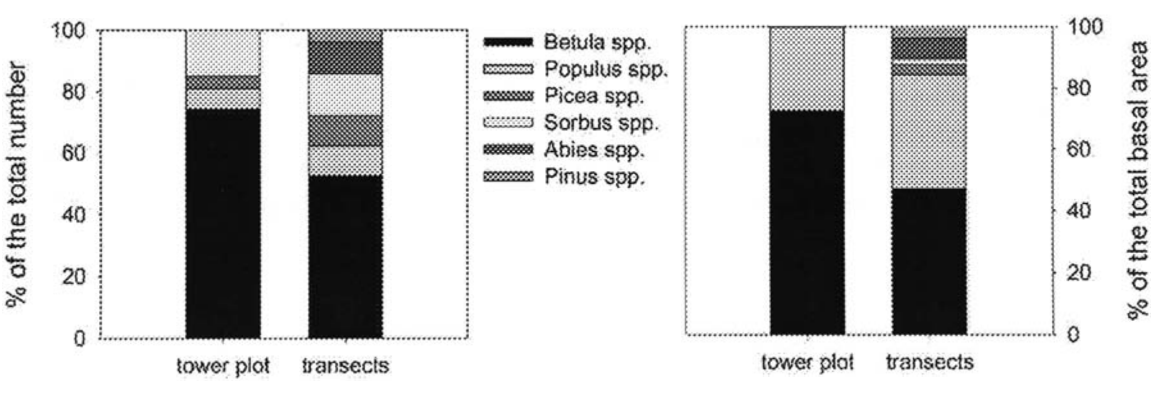

(A)

(B)

Fig. 2. Species distribution (A) and basal area distribution (B) of living trees.

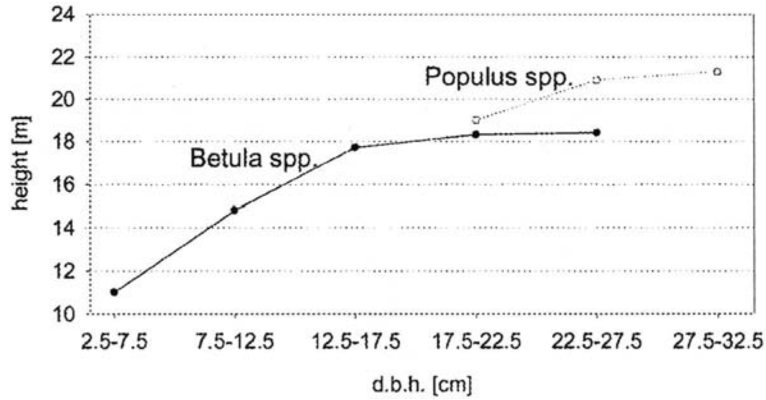

Fig. 3. Heights distribution of *Betula* spp. and *Populus* spp. in breast height diameter (d.b.h.) classes of 5 cm.

(at b.h.) was 29 m^2 ha^{-1} and mean tree diameter was 11.3 cm.

The vertical structure of the canopy, as mentioned before, is stratified in more layers. The dominant layer is constituted by *P. tremula* L. trees (Fig. 3) spatially clumped with total crown coverage less than 30%. The sub-dominant layer is a homogeneous and uniform layer of birch crowns. The different vertical distribution of birch and aspen is explained by the highest growth rate of aspen that is able to compete for light more favourably than birch.

The lower canopy is constituted by *S. sibirica, A. sibirica, P. obovata,* and a regeneration layer. The dominated layer, which is composed by trees older then 20 years, occupies a range of heights between 2 and 6 m, and has a sparse distribution.

The regeneration (Fig. 4, referring to 'tower plot'), which does not reach the height of 1.30 m, is abundant but not dense.

In the regeneration and in the dominated layer the birch is completely absent, while the aspen is still able to have a sparse regeneration.

2.2. Flux measurements

Exchange rates of sensible heat, water vapour and carbon dioxide have been determined by *eddy covariance technique* (e.g. Baldocchi et al., 1988).

Basically the eddy flux of a given scalar c (i.e. CO_2) is given by

$$F_c = \rho\overline{w'c'}$$

where w' is the vertical wind speed fluctuation around the mean, c' the scalar concentration fluctuation around the mean and p the density of dry air.

A scaffold tower was erected in the middle of the stand. At a height of 24 m a three-dimensional sonic anemometer (Metek, DE) and the air inlet of the

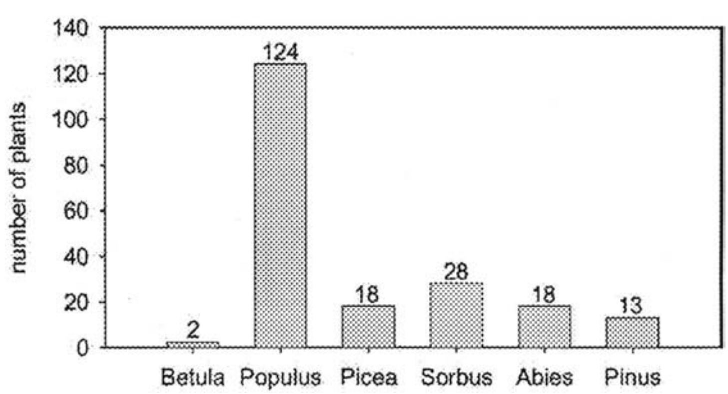

Fig. 4. Species distribution of stand core regeneration (trees shorter than 1.30 m), plot area = 25 m × 25 m.

CO_2/H_2O infrared gas analyser (Licor, USA) were positioned, the main canopy height being 18 m.

The footprint peak (distance of the maximum of the distribution function of flux contribution in upwind direction) and the 70% of the footprint (distance in upwind direction at which the cumulated distribution function of flux contribution is 0.7), calculated according to Schuepp et al. (1990), were 19 and 109 m, respectively.

The intake of the 22 m tube (0.4 cm of internal diameter) was protected with a Gelman filter (2 μm). Flow rate was stabilised between 7 and 8 l min^{-1}, so that air movement in the tube might be considered turbulent (sample line Reynolds number Re = 2475 at air temperature = 20 °C and flow rate = 7 l min^{-1}) assuming a threshold of about Re = 2030 for transition to turbulent flow (Aubinet et al., 2000).

Calibration of infrared gas analyser was carried out every 15 days by means of reference gases. Mass and energy fluxes have been calculated according to EUROFLUX methodology (Aubinet et al., 2000) and applying a linear detrend algorithm to eddy data (Gash and Culf, 1996).

Fluxes have been corrected for the storage using a discrete representation (Greco and Baldocchi, 1996): canopy CO_2 storage was calculated using the time change of CO_2 concentration at reference height, assuming a homogeneous vertical profile distribution.

Air temperature (above and within the canopy), rainfall, net radiation (installed at 24 m), photosynthetic photon flux density (PPFD) (above and below the canopy), heat flux in the soil (at two locations with heat flux plates installed at depth of 0.05 m) and soil temperature (installed at depth of 0.05 and 0.30 m) were measured.

Data were taken continuously from early July to late August 1999. Owing to the harsh environmental conditions, the system experienced some breakdowns and the missing data, due to system failure, calibration and maintenance, accounted for the 29% of all half-hour values. Hourly gaps of data (up to 2 h) were filled via interpolation between earlier and later measurements. Larger gaps were filled by using empirical regression with meteorological data or by replacing the missing observation with the average for that half-hour, based on adjacent days (7 days windows size), in case meteorological data would not be available either.

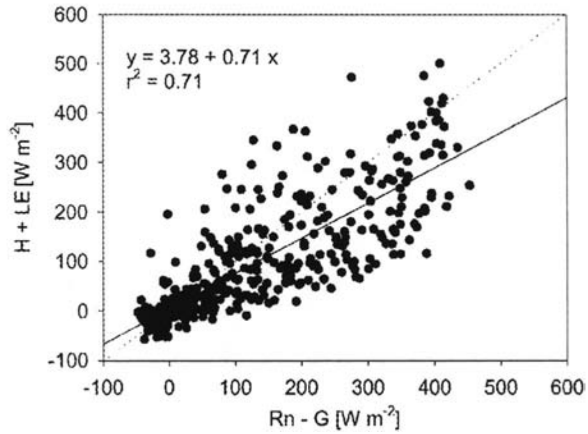

Fig. 5. Energy balance closure (daytime half-hourly values) for the whole measurement period, coefficients describing the linear regression function fitting the data points are reported.

The plausibility of eddy data was assessed comparing turbulent heat fluxes (H and LE) with the available energy flux (net radiation, R_n, and heat flux in the soil, G). In the energy balance closure test of Fig. 5 (values refer to the whole measurement period), daytime (PPFD ≥ 30 μmol m^{-2} s^{-1}) sums of sensible and latent heat were plotted against total available radiation energy minus ground heat flux. The slope of linear regression fitting the data points of the scatter plot in Fig. 5 corresponds to the energy balance closure, which is limited to about 30% of the theoretical value (slope = 1). The underestimation of the energy closure is a rather common feature of several *eddy covariance* papers (Aubinet et al., 2000). The point is still at issue and our results generally fail into the same range of error.

Data quality was checked by means of footprint analysis and energy balance closure (above). No rejection criterion was assumed for night time fluxes.

3. Results and discussion

3.1. Energy dissipation and partitioning

The birch stand dissipated more energy via evapotranspiration with a mean Bowen ratio of about 0.4. This energy partitioning might be explained with the large amount of water available resulting from the spring snowmelt (unusual low temperatures in May

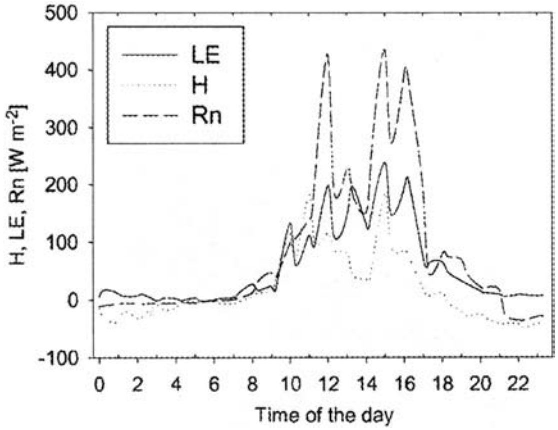

Fig. 6. Typical daily trend of latent heat (LE), sensible heat (*H*) and net radiation (R_n)-15 August.

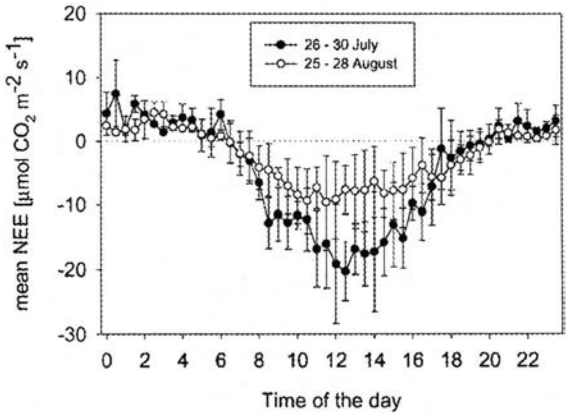

Fig. 7. Average daily courses of ecosystem carbon exchange rates of the regenerating forest in two periods of July and August, bars represent standard errors of the means.

and June delayed the snowmelt, thus leaving a significant amount of free water available for evaporation). Mean Bowen ratio increased from July to August, according to the free water availability decrease, 0.15 in July and 0.53 in August. A typical daily trend of *H*, LE (sensible and latent heat, measured by *eddy covariance)* and R_n (net radiation, measured by net radiometer sensor) is showed in Fig. 6, referring to 15 August (with a mean Bowen ratio of 0.75).

3.2. Carbon exchange

The carbon flux between a forest and the atmosphere, as measured by *eddy covariance technique,* equals the NEE, where NEE is the sum of the contribution of different processes: gross photosynthesis and respiration associated with leaves, wood construction and maintenance, roots and microbes.

For consistency with micrometeorological sign convention, CO_2 uptake from the vegetation is negative, whereas a net CO_2 release to the atmosphere is positive.

Typical daily trends of the forest NEE are presented in Fig. 7. During the period of maximum uptake (days 26-30 July) the CO_2 flux density peaks at about 12 h (minimum exchange rate, day 26 July, is -35 µmol m^{-2} s^{-1}) in parallel with PPFD.

During the late vegetative season (days 25-29 August) maximum CO_2 uptake is reduced (minimum exchange rate is -17 µmol m^{-2} s^{-1}, day 25 August) reflecting a reduced photosynthetic activity. A reduction in night time respiration (assuming that measured fluxes might reproduce the real courses of respiratory fluxes) could be explained with the decrease of air temperature in late August.

Daily maximum uptake from the vegetation and integrated carbon uptake are decreasing at the end of the vegetative season (see Fig. 8, daily NEE, sums of half-hourly values).

Cumulative carbon flux for the whole measurement period is presented in Fig. 9. Note that the zero refers to the beginning of the measurement period (it is not a true zero point). From Fig. 9 it can be seen that the

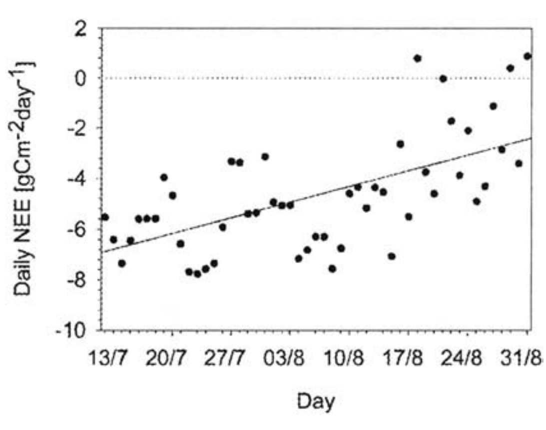

Fig. 8. Daily NEE, the line (linear regression function fitting the data points) shows a decreasing trend.

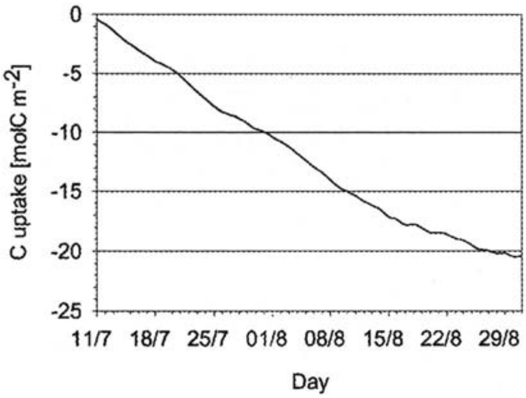

Fig. 9. Cumulative NEE over the period 11 July 1999 to 31 August 1999 for the regenerating forest investigated.

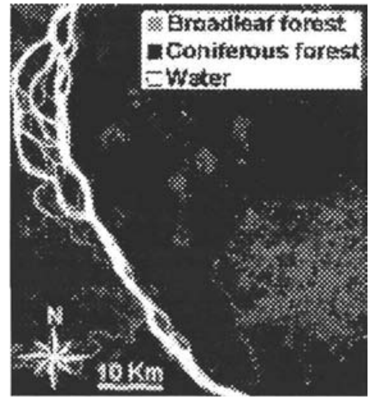

Fig. 10. Satellite classification: segmentation of the study area into three major land use-land cover classes.

stand is a significant sink of carbon. In the measurement period (52 days) the ecosystem sequestered 246 g C m^{-2} (897 g CO_2 m^{-2}).

The sink strength of this broadleaf forest appears considerably higher than the one of evergreen forests (Scots pine) in the same area (Shulze et al., 1999; Valentini et al., 2000). Although a comprehensive analysis of the differences between evergreen coniferous and broadleaves deciduous forests in terms of cumulative NEE has not yet been effected, the present study seems to indicate that the higher rates of carbon exchanges of birch are consistent with their role in terms of ecological succession, since the birch is a rather competitive species in the first establishment period after fire under good site conditions.

3.3. Spatial analysis

A Landsat-4 TM scene that includes the *eddy covariance* study site, was used as investigation area. In order to separate the dominant broadleaf succession stages (Furyaev et al., 1983) from the coniferous stages, a supervised classification of the *dark coniferous taiga* area, east of Yenisey River, was performed (Fig. 10). Ground truths were collected in a field campaign in order to test the classification results. Satellite image was georeferenced according to local topographic map with simple polynomial equation (the area is flat enough to avoid more complicated orthorectification methods). Since the goal of this remote sensing analysis was a single classification,

Table 2
Land use-land cover classification results

Type of forest	Area (km^2)
Dark coniferous taiga	315
Broadleaf forest	63

we assumed horizontal homogeneity of the atmosphere (the acquired image was totally cloud and haze free) and no atmospheric correction was performed. Classification accuracy was tested against a truth map created with the visual interpretation of some satellite declassified intelligence images (CORONA project), and resulted in a 0.93 value of KIA (kappa index of agreement, Rosenfield and Fitzpatric-Lins, 1986).

The result of the spatial analysis (Table 2) indicates that the dominant broadleaf succession forest stages represent 22% of the *dark coniferous taiga area.* Thus, in the hypotheses that only fire can generate a broadleaf forest (Furyaev et al., 1983), the spatial frequency of burnt areas might be assumed to amount to the same rate (22%).

4. Conclusions

Broadleaf regenerating forests, generated by large area disturbances (fires), represent a contrasting vegetation cover in the Siberian *dark coniferous taiga* landscape. The measured Bowen ratios for the regenerating forest site were very low compared with other evergreen forests in the area (Shulze et al., 1999). Alternation of this kind of broadleaf forests with evergreen forests dissipating more energy via sensible heat may enhance convective precipitation, thunderstorms, lightning and then natural fire disturbance as suggested by Valentini et al. (2000).

Spatial frequency of burnt areas, amounts to the 20% of the investigated area (see Section 3.3). Analysis of carbon exchanges of the investigated stand (in the measurement period, 52 days, 246 g C m^{-2} were sequestered from the atmosphere) suggests that this kind of regenerating forest is a significant sink of carbon.

The rather high crown fire occurrence and the strong carbon sequestration properties of the post fire regenerating forests in the *dark coniferous taiga* underline the importance of large-area disturbances in the boreal forest carbon budget.

Acknowledgements

This study was supported by EU, Eurasia-net project, Contract no. ENV4-CT98-0797 (DG 12-EHKN). We thank Prof. E. Vaganov and all the people of the Forest Institute of Krasnojarsk for the valuable support and guidance during the scientific campaigns.

References

Aubinet, M., Grelle, A., Ibrom, A., Rannik, Ü., Moncrieff, J., Foken, T., Kowalski, A.S., Martin, P.H., Berbigier, P., Bernhofer, C., Clement, R., Elbers, J., Granier, A., Grünwald, T., Morgenstern, K., Pilegaard, K., Rebmann, C., Snijders, W., Valentini, R., Vesala, T., 2000. Estimates of the annual net carbon and water exchanges of forest: the EUROFLUX methodology. Adv. Ecol. Res. 30, 113-175.

Baldocchi, D.D., Hicks, B.B., Meyers, T.P., 1988. Measuring biosphere-atmosphere exchanges of biologically related gases with micrometeorological methods. Ecology 69, 1331-1340.

Furyaev, V.V., Wein, R.W., MacLean, D.A., 1983. Fire influences in Abies dominated forest. In: The Role of Fire in the Northern Circumpolar Ecosystem. Wiley, pp. 221-234.

Gash, J.H.C., Culf, A.D., 1996. Applying a linear detrend to eddy correlation data in real time. Boundary-Layer Meteorol. 79, 301-306.

Greco, S., Baldocchi, D.D., 1996. Seasonal variations of CO_2 and water vapour exchange rates over a temperate deciduous forest. Global Change Biol. 2, 183-197.

Melillo, J.M., McGuire, A.D., Kicklighter, D.W., Moore III., B., Vorosmatry, C.J., Schloss, A.L., 1993. Global climate change and terrestrial net primary production. Nature 363, 234-240.

Nilsson, S., Shvidenko, A., 1997. The Russian Forest Sector. IIASA Working Paper. International Institute for Applied Systems Analysis, Laxenburg, Austria.

Rosenfield, G.H., Fitzpatric-Lins, K., 1986. A Coefficient of agreement as a measure of thematic classification accuracy. Photogr. Eng. Remote Sensing 52, 2.

Schimel, S.D., 1995. Terrestrial ecosystems and the carbon cycle. Global Change Biol. 1, 77-91.

Schuepp, P.H., Leclerc, M.Y., MacPherson, J.I., Desjardins, R.L., 1990. Footprint prediction of scalar fluxes from analytical solutions of the diffusion equation. Boundary-Layer Meteorol. 50, 355-373.

Shulze, E.D., Lloyd, J., Kelliher, F.M., Wirth, C., Rebman, C., Luhker, B., Mund, M., Knohl, A., Milyukova, I.M., Schulze, W., Ziegler, W., Varlagin, A.B., Sogachev, A.F., Valentini, R., Dore, S., Grigoriev, S., Kolle, O., Panfyrov, M.I., Tchebakova, N., Vygodskaya, N.N., 1999. Productivity of forests in the Eurosiberian boreal region and their potential to act as carbon sink - a synthesis. Global Change Biol. 5, 703-722.

Shvidenko, A., Nilsson, S., 1994. What do we know about the Siberian forests? Ambiology 23 (7), 396-404.

Tans, P.P., Fung, I.Y., Takahashi, T., 1990. Observational constraints on the global CO_2 budget. Science 247, 1431-1438.

Valentini, R., Dore, S., Marchi, G., Mollicone, D., Panfyorov, M., Rebmann, C., Kolle, O., Schulze, E.D., 2000. Carbon and water exchanges of two contrasting central Siberia landscape types: regenerating forest and bog. Funct. Ecol. 14, 87-96.